CrossCLR: Cross-modal Contrastive Learning For Multi-modal Video Representations

Mohammadreza Zolfaghari[1*], Yi Zhu[2], Peter Gehler[2], Thomas Brox[2]

[1]University of Freiburg   [2]Amazon

Abstract

Contrastive learning allows us to flexibly define powerful losses by contrasting positive pairs from sets of negative samples. Recently, the principle has also been used to learn cross-modal embeddings for video and text, yet without exploiting its full potential. In particular, previous losses do not take the intra-modality similarities into account, which leads to inefficient embeddings, as the same content is mapped to multiple points in the embedding space. With CrossCLR, we present a contrastive loss that fixes this issue. Moreover, we define sets of highly related samples in terms of their input embeddings and exclude them from the negative samples to avoid issues with false negatives. We show that these principles consistently improve the quality of the learned embeddings. The joint embeddings learned with CrossCLR extend the state of the art in video-text retrieval on Youcook2 and LSMDC datasets and in video captioning on Youcook2 dataset by a large margin. We also demonstrate the generality of the concept by learning improved joint embeddings for other pairs of modalities.

1. Introduction

Cross-modal tasks, especially tasks connecting video and text, expand the influence and applicability of computer vision. It enables, for example, video retrieval based on text queries [11, 10, 24], image and video captioning [12], and exploitation of text-based meta-data for visual feature learning [26, 28, 57, 41]. Linking the different, not directly comparable sources of data creates new challenges that do not appear in visual-only learning.

In this paper, we consider cross-modal contrastive learning and introduce a loss that relates the data in a more efficient manner than direct adoption of a loss designed for vision-only data. Contrastive learning is based on the definition of positive and negative samples relative to an ankor point, which yields a flexible principle: pull together an anchor and a positive sample in the embedding space, and push apart the anchor from many negative samples. Many implementations of this principle have been proposed: max-margin loss [14], triplet loss [46, 47, 18],
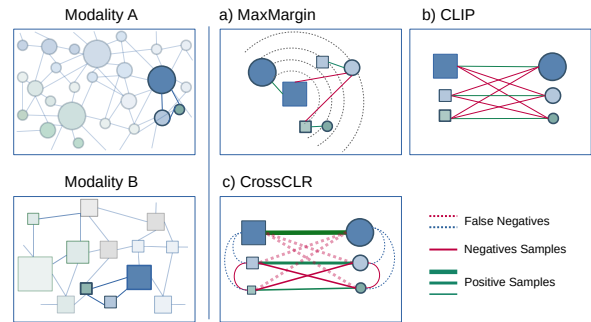
*Work done during an internship at Amazon Tübingen.

Figure 1. When learning a joint embedding between two modalities A and B, existing contrastive learning losses, such as Max-Margin [11, 24] and CLIP [34], ignore the possibility of false negative samples and, thus, push semantically related concepts apart. The proposed CrossCLR loss indentifies influential samples (large circles/boxes), removes them from the negative set and increases their weight in the minibatch. Moreover, CrossCLR adds intra-modal links to the loss.

and InfoNCE [44]. Usually positive pairs are defined as synthetic, spatial [3, 33], or temporal variations of an instance [33]. Instance discrimination has been applied also to cross-modal tasks, where positive pairs (or a set of positives) are sampled from the same time window (MIL-NCE [26], AVSA [30], CM-ACC [25]).

In this paper, we investigate two issues of existing cross-modal contrastive learning techniques. **1.** The cross-modal loss only ensures that the features from the two modalities map to proximate points in the joint embedding, but they lack an explicit measure that also ensures that similar features from the same modality stay close-by in the joint embedding. In previous works, it is implicitly presumed that the similarity between modalities, via transitivity, will also preserve similarity within the modality. However, it has not been shown that this is the case[1]. If similar features from the same modality map to far-apart points in the joint embedding, the embedding lacks semantic meaning and, thus, will generalize badly. **2.** The focus of previous cross-

[1]Since many previous works focus on unsupervised feature learning rather than learning joint embeddings, they do not assume that the input embeddings are meaningful, in the sense that semantically related concepts are initially close-by in the feature space. Therefore, preservation of input similarities is meaningless to them. In this work, we do assume that the input embeddings for each modality (e.g. ImageNet pretrained features) already cover some semantics, and we target a joint embedding that leverages these semantics across modalities.

modal contrastive losses is on the definition of positive pairs, whereas negative samples are randomly drawn from the entire distribution. This does not reflect the effect of what we call *influential samples* – samples that are similar to many other samples and, thus, have a large influence on the shape of the embedding. Marking influential samples as negatives will likely push apart samples that are actually strongly related.

As a remedy to the first problem, we propose a contrastive loss that enforces the joint embedding to respect the similarity of samples in the original features spaces. Moreover, as a remedy to the second problem, we define influential samples as samples with a high connectivity within the dataset and remove these samples from the set of negatives. We also introduce a loss weighting based on the connectivity. We show that all three measures lead to an improved cross-modal embedding as tested in terms of video-text retrieval and video captioning. While this paper focuses on video and text as modalities, we show that the positive effects of the proposed cross-modal loss generalizes to other pairs of modalities.

2. Related Work

2.1. Sample Selection in Contrastive Learning

Different from the recent research [3, 16, 6, 5, 13, 2], our work addresses multi-modal contrastive learning. We propose inter- and intra-modality loss objectives to ensure that samples with similar content stay close in the joint embedding space, regardless of the modality. However, sample selection plays an important role in contrastive learning. Inspired by Khosla et al. [20], Zhang et al. [38] proposed an adaptive self-supervised learning technique to mine nearest positive samples without using label information. Han et al. [15] introduced a co-training method to mine hard positive samples by using other complementary views of the data for video representation learning. In terms of negative sampling, recent work explored informative (hard) negatives to facilitate better and faster contrastive learning [19, 36].

Our work also focuses on selecting better negative samples, but instead of mining hard negatives, we introduce the concept of influential samples. We define these as samples that are strongly connected with others and more likely lead to semantic collision. We exclude them from the negative set and give them more weight in the loss.

2.2. Multi-modal Representation Learning

Video data often consists of multiple modalities, such as raw RGB, motion, audio, text, detected objects, or scene labels. Employing multiple of these together helps better understand the content of video [26, 11]. Recently, transformer-based models for cross-modal representation learning became popular [11, 12, 34]. VideoBERT [41] adopted the BERT design and applied it on quantized

video representations. Miech et al. [28] introduced the HowTo100M dataset. Later work exploited the noisy pairings of this dataset for pretraining video-language models [26, 57]. MIL-NCE [26] proposed to consider multiple positive pairs sampled in a temporally close neighborhood to tackle the misaligned video narrations.

While the above works focus on learning representations from scratch exploiting very large datasets, another line of research is to learn a joint embedding given pre-trained expert models to compute the input features [24, 11, 27]. Miech et al. [27] computed features from pre-trained experts for text-to-video retrieval. The overall similarity is a weighted sum of each individual expert's similarity score. CE [24] proposed a mixture of experts model and a collaborative gating mechanism to combine experts. A recent extension (MMT) [11] extracts the expert features from 7 different domains and employs a time-aware modality aggregation mechanism. MMT incorporates a bidirectional max-margin ranking loss for training.

Our work belongs to the second group of works, where we assume pre-trained input embeddings. CrossCLR overcomes the limitations of max-margin ranking and contrastive learning losses by enforcing consistency within each modality. It avoids pushing away semantically similar representations in the joint embedding space by introducing and exploiting influential samples.

3. CrossCLR

In this section, we first define the cross-modal learning task and highlight the issues that normal contrastive learning faces when learning a cross-modal embedding. Then we introduce modifications to the contrastive loss to ensure intra-modal alignment and to avoid semantic collision.

Cross-modal alignment. Cross-modal alignment aims to learn two encoders $f_x(\cdot)$ and $f_y(\cdot)$ that map embeddings x and y of two modalities A and B to $z_x = f_x(x)$ and $z_y = f_y(y)$, such that z_x and z_y are close to each other in the learned embedding space if they refer to similar content, otherwise far away. That means, it aims to learn a similarity function between samples from A and B. Given a sample pair (x_i, y_i), which is assumed to describe similar content. For example, x_i and y_i can be the embeddings of a video clip and a corresponding text description of its content, respectively. A successfully learned cross-modal similarity is supposed to generalize to unseen pairs, notwithstanding the typically large variation in the input modalities A and B even when they show similar content. A and B can be arbitrary modalities. In this paper, we assume samples from A to be a feature embedding derived from a video clip and samples from B to be a feature embedding of a sentence. However, we also show an experimental study where A and B are different modalities derived from a video clip.
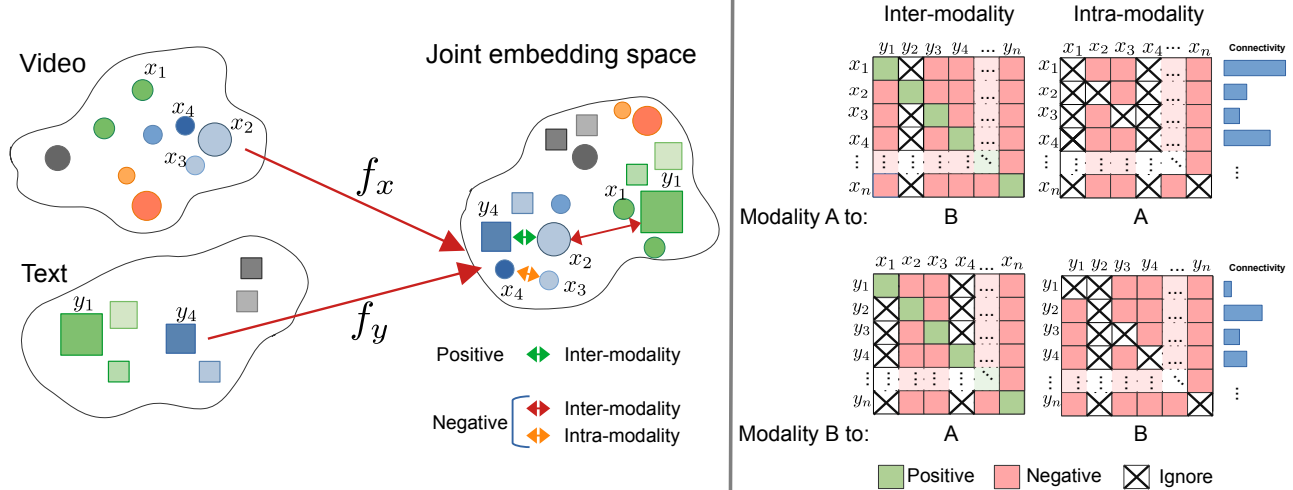
Figure 2. CrossCLR loss. We first find the influential samples. Influential samples are similar to a large set of other samples. We emphasize these samples in the loss. Additionally, we prune these samples from the negative set, because we want to prevent the loss to falsely push them apart while they share semantics with other samples.

Pretrained feature experts. We encode feature representations from videos, such as action, appearance, object using off-the-shelf feature extractors [11, 27, 29, 24]. Each expert is a pre-trained model on a specific task, more details in Section 4.2. Given a video v, we sample m frames and feed them to the expert model to obtain per-frame expert features $x = [e_1, \ldots, e_m]$. For text data, we use *BERT-Base uncased* model as feature extractor.

To align embeddings of modality A to embeddings of modality B, we follow the two-stream hierarchical architecture of COOT [12], as shown in Fig.4. It consists of a local transformer for clip-level embeddings and a global transformer for video-level embeddings. Given frame/word-level expert features, we obtain the clip/sentence level embeddings via the local transformer. These local embeddings serve as input to the global transformer, which yields the final video/paragraph representation.

Contrastive learning. The sample pairs (x_i, y_i) give us information for contrastive learning. In particular, each such sample i can be regarded as a positive pair, whereas all pairs (x_i, y_j) for $j \neq i$ will be regarded as negative pairs. To be precise, for each sample x_i in the minibatch $\mathcal{M}$, the positive set P_i and negative set N_i are defined as $\mathsf{P}_i = \{y_i\}$ and $\mathsf{N}_i = \{y_j | \forall y_j \in \mathcal{M}, j \neq i\}$. The corresponding contrastive loss on a minibatch $\mathcal{M}$ is:

$$L = \mathbb{E}_{i \in \mathcal{M}} \left[-\log \frac{\exp(f_x(x_i)^T f_y(y_i))}{\exp(f_x(x_i)^T f_y(y_i)) + \sum\limits_{y_j \in \mathsf{N}_i} \exp(f_x(x_i)^T f_y(y_j))} \right], \quad (1)$$

which is being optimized w.r.t. the parameters of the encoders f_x and f_y.

One weakness in this formulation is the ad-hoc definition of negative samples. We simply assumed that all combinations (x_i, y_j) with $i \neq j$ have dissimilar content. However, this is not always the case. For instance, two

sentences "someone drinks a cup of tea", and "she talks on the phone while drinking tea", aligned with two different video clips i and j have largely overlapping content. The loss objective in equation (1) will only be minimized if $f_x(x_i)$ and $f_y(y_j)$ are mapped to different points in the embedding, despite their high semantic similarity. Moreover, nothing in the above loss enforces that $f_y(y_i)$ and $f_y(y_j)$ are mapped to proximal points in the joint embedding space, even when y_i and y_j are similar in their original embedding space, as in the given example.

3.1. Inter-Modality and Intra-Modality Alignment

Let us first approach the missing alignment of the input modalities in the joint embedding. If we assume, like in this paper, that the input modalities have already passed an encoder network that is able to place semantically related inputs nearby in the original feature embedding, we should preserve this proximity also in the joint embedding space. Therefore, $f_x(\cdot)$ and $f_y(\cdot)$ should be optimized not only to map x_i and y_i of a pair (x_i, y_i) to a proximate location in the joint embedding (inter-modality), but similar samples x_i and x_j from the same modality should be mapped in close proximity (intra-modality). The inter-modality and intra-modality negative sets for sample x_i are defined as: $\mathsf{N}_i^E = \{y_j | \forall y_j \in \mathcal{M}, j \neq i\}$ and $\mathsf{N}_i^R = \{x_j | \forall x_j \in \mathcal{M}, j \neq i\}$.

Therefore, the learning objective is based on four contrastive components including A-to-B, A-to-A, B-to-A, and B-to-B alignments, as shown in Fig. 2-Right:

$$L(x_i) = -\log \frac{\delta(x_i, y_i)}{\delta(x_i, y_i) + \underbrace{\sum\limits_{y_j \in \mathsf{N}_i^E} \delta(x_i, y_j)}_{\text{Inter modality negative pairs}} + \lambda \underbrace{\sum\limits_{x_j \in \mathsf{N}_i^R} \delta(x_i, x_j)}_{\text{Intra modality negative pairs}}}, \quad (2)$$
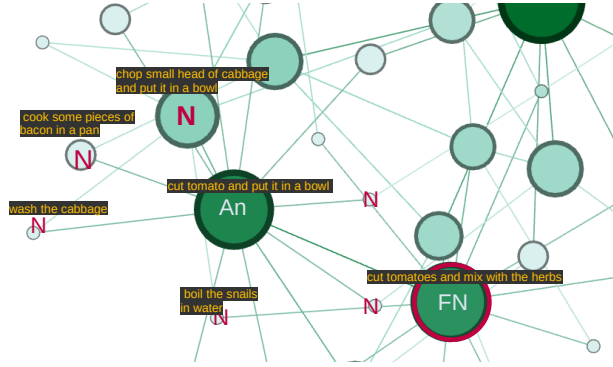
3

Figure 3. Example of influential text samples in the Youcook2 dataset (darker green -> more vital). An: Anchor sample, FN: False negative, N: Negative sample.

$$L(y_i) = -\log \frac{\delta(y_i, x_i)}{\delta(y_i, x_i) + \underbrace{\sum_{x_k \in \mathsf{N}_i^E} \delta(y_i, x_j)}_{\text{Inter modality negative pairs}} + \lambda \underbrace{\sum_{y_j \in \mathsf{N}_i^R} \delta(y_i, y_j)}_{\text{Intra modality negative pairs}}}, \quad (3)$$

where $\delta(x_i, y_j) = \exp(f_x(x_i)^T f_y(y_j)/\tau) = \exp(z_{x^i}^T z_{y^j}/\tau)$. The second and the third term in the denominator sum up inter-modal and intra-modal negative samples, respectively. λ is a hyper-parameter to control intra-modality alignment. We apply ℓ_2-normalisation to the input feature embeddings before computing the inner product [40, 48, 34]. In such case, the inner product is equivalent to cosine similarity. While the nominator is symmetric, the denominator is not. Hence, we add up two losses for each sample pair (x_i, y_i) – one for each modality.

3.2. Avoiding Semantic Collision

The second issue we identified with regular contrastive learning is the contrasting of false negative samples that have actually strong semantic overlap. The common assumption in contrastive learning is that a large enough number of negative samples help to learn better representations, because in each training batch, the model contrasts more semantic representatives. However, Arora et al. [1] showed that this assumption does not always hold. When there is a large number of negative samples, the chance of observing negative samples with high semantic overlap increases. As shown in Figure 3, both samples *"cut tomato and put it in a bowl"* and *"cut tomatoes and mix with the herbs"* are considered negative samples in standard contrastive learning methods. By contrasting these undesirable negative pairs, the network is encouraged to discard their common features in the learned embedding, which is, in fact, the common semantic content, e.g., similar objects and actions in two videos; see also Figure 3. We call this issue *semantic collision*, which is known as "class collision" in Arora et al. [1, 39] and "sampling bias" in Chuang et al. [7] in a different context. When there is a large number of negative samples, frequent semantic collisions can prevent

---

Algorithm 1 CrossCLR's learning algorithm.

input: batch size N, queue Q, constants τ, κ, and λ, networks f_x and f_y for modality A and modality B.
define $\delta(x_i, y_j)$ **as:**
$$\delta(x_i, y_j) = e^{(\frac{f_x(x_i)^T f_y(y_j)}{\tau})} = e^{(\frac{z_{x_i}^T z_{y_j}}{\tau})}$$
for sampled minibatch $\{x_i, y_i\}_{i=1}^N$ **do**
  Queuing $\{x_i, y_i\}_{i=1}^N$ in Q and dequeuing oldest keys;
  for all $k \in \{1, \dots, |Q|\}$ **do**
  $$c_{x_k} = \frac{1}{|Q|} \sum_{x_j \in Q} \frac{x_k^\top x_j}{||x_k|| \cdot ||x_j||}$$
  $$c_{y_k} = \frac{1}{|Q|} \sum_{y_j \in Q} \frac{y_k^\top y_j}{||y_k|| \cdot ||y_j||}$$
  if $c_{x_k} < \gamma$ **then:** $\hat{\mathsf{N}}_x^{IR} \leftarrow \hat{\mathsf{N}}_x^{IR} \cup x_k$ **end if**
  if $c_{y_k} < \gamma$ **then:** $\hat{\mathsf{N}}_y^{IR} \leftarrow \hat{\mathsf{N}}_y^{IR} \cup y_k$ **end if**
  end for
  for all $i \in \{1, \dots, N\}$ **do**
  $$\alpha_{x_i} = \frac{1}{|Q|} \sum_{x_j \in Q} \frac{x_i^\top x_j}{||x_i|| \cdot ||x_j||}$$
  $$\alpha_{y_i} = \frac{1}{|Q|} \sum_{y_j \in Q} \frac{y_i^\top y_j}{||y_i|| \cdot ||y_j||}$$
  if $\alpha_{x_i} < \gamma$ **then:** $\hat{\mathsf{N}}_x^{IE} \leftarrow \hat{\mathsf{N}}_x^{IE} \cup y_i$ **end if**
  if $\alpha_{y_i} < \gamma$ **then:** $\hat{\mathsf{N}}_y^{IE} \leftarrow \hat{\mathsf{N}}_y^{IE} \cup x_i$ **end if**
  $$w_{x_i} = e^{(\frac{\alpha_{x_i}}{\kappa})}; w_{y_i} = e^{(\frac{\alpha_{y_i}}{\kappa})}$$
  $$L_{x_i} = -w_{x_i} \log \frac{\delta(x_i, y_i)}{\delta(x_i, y_i) + \sum_{y_k \in \hat{\mathsf{N}}_x^{IE}} \delta(x_i, y_k) + \lambda \sum_{x_k \in \hat{\mathsf{N}}_x^{IR}} \delta(x_i, x_k)}$$
  $$L_{y_i} = -w_{y_i} \log \frac{\delta(y_i, x_i)}{\delta(y_i, x_i) + \sum_{x_k \in \hat{\mathsf{N}}_y^{IE}} \delta(y_i, x_k) + \lambda \sum_{y_k \in \hat{\mathsf{N}}_y^{IR}} \delta(y_i, y_k)}$$
  end for
  update networks f_x and f_y to minimize $L = \frac{L_x + L_y}{2}$
end for
return encoders $f_x(\cdot)$ and $f_y(\cdot)$

---

the algorithm from learning good representations.

We argue that it is important to reduce the effect of semantic collision and remove false negatives from the negative set. This is non-trivial, since we do not have direct information, e.g., which of the samples are false negatives. To this end, we introduce the concept of *influential samples* and propose two components based on influential samples: negative set pruning and loss weighting.

Influential samples. We assume that samples that are strongly connected with other samples are more likely to share semantics and, thus, more likely lead to semantic collision. We use a queuing technique to store data samples. This allows us to compute more reliable semantic similarity scores. Also recent studies [49, 6, 16], showed that a large set of negatives is critical in contrastive representation learning. The queue size can be much larger than the mini-batch size and we update it progressively by replacing the oldest mini-batch with the current mini-batch. Hence, given a collection of M samples in queue $\mathcal{Q}_x = \{x_n\}_{n=1}^M$, we define an influential sample as a sam-

4

ple x_i that is strongly connected with many other samples in $\mathcal{Q}_x$, where we measure connectivity $C(x_i)$ by the aggregated similarity of features:

$$C(x_i) = \frac{1}{M} \sum_{j=1}^{M} \frac{x_i^{\top} x_j}{||x_i|| \cdot ||x_j||} \quad (4)$$

The higher the connectivity, the more influential the data sample is. Influential samples tend to be either in the center of a semantic cluster or establish a link between clusters, as shown in Fig. 3. We use the connectivity of each sample for pruning and weighting.

Negative set pruning. The connectivity of samples can be thresholded to identify influential samples $\mathcal{I}_x$. Given a collection of samples $\mathcal{Q}_x$ and threshold γ, we define $\mathcal{I}_x$ as $\mathcal{I}_x = \{x_i | C(x_i) > \gamma, \forall x_i \in \mathcal{Q}_x\}$. To reduce the described effect of false negatives in contrastive learning, we remove all influential samples (in each modality) from the negative set. Therefore, we redefine the inter-modality and intra-modality negative sets as: $\hat{\mathsf{N}}_x^E = \{y_j | \forall (x_j, y_j) \in \mathcal{M}, x_j \notin \mathcal{I}_x\}$ and $\hat{\mathsf{N}}_x^R = \{x_j | \forall x_j \in \mathcal{Q}_x, x_j \notin \mathcal{I}_x\}$. This is also illustrated in Fig.2-Right.

Loss weighting. Moreover, we suggest using the connectivity to emphasize samples with large aggregated connectivity over those with low connectivity. Samples with very low connectivity can be regarded as outliers to the dataset. They are too sparse to positively influence the shape of the embedding. Thus, we reduce their influence on the representation learning. At the same time, we increase the weight of influential samples, since the cross-modal information of these samples should have a large impact on the shape of the embedding. In particular, for each sample and modality we introduce a weight

$$w(x_i) = \exp(C(x_i)/\kappa), \quad (5)$$

where κ is a hyperparameter. While we defined the connectivity, the influential samples, and the weights for modality A, the same applies for modality B.

The final CrossCLR loss is $(L_x + L_y)/2$ with

$$L_x = -\mathbb{E}_{i \in \mathcal{M}} \left[w(x_i) \log \frac{\delta(x_i, y_i)}{\delta(x_i, y_i) + \sum_{y_k \in \hat{\mathsf{N}}_x^E} \delta(x_i, y_k) + \lambda \sum_{x_k \in \hat{\mathsf{N}}_x^R} \delta(x_i, x_k)} \right] \quad (6)$$

$$L_y = -\mathbb{E}_{i \in \mathcal{M}} \left[w(y_i) \log \frac{\delta(y_i, x_i)}{\delta(y_i, x_i) + \sum_{x_k \in \hat{\mathsf{N}}_y^E} \delta(y_i, x_k) + \lambda \sum_{y_k \in \hat{\mathsf{N}}_y^R} \delta(y_i, y_k)} \right] \quad (7)$$

4. Experiments

4.1. Datasets and Metrics

We conducted experiments on LSMDC [37] and Youcook2 [55] datasets.

LSMDC [37] contains 118,081 short video clips extracted from 202 movies. Each clip is annotated with a
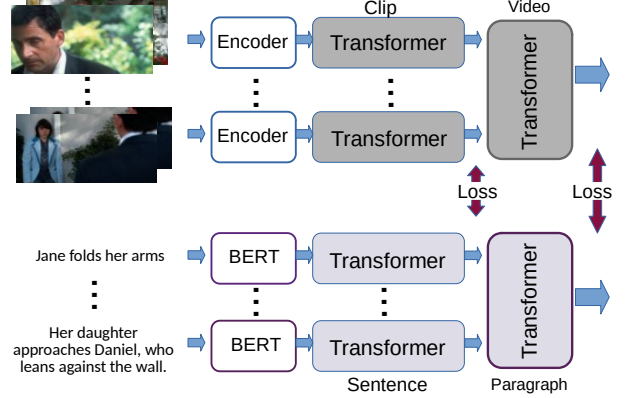

Figure 4. **Architecture.** The model consist of two branches: one for modality A (e.g. Video) and one for modality B (e.g. Text). Each modality is represented by features from a pretrained expert, which we keep frozen (visual Encoder and BERT). These embeddings are fed into a transformer, which maps the input features into a joint embedding space. For video and text, we use a two-level hierarchy of transformers, where the loss is applied at the clip/sentence-level and at the video/paragraph level. The second stage takes the features from the joint embedding of the first transformer as input.

caption, extracted from either the movie script or the audio description. The test set is composed of 1000 videos, from movies not present in the training set.

Youcook2 [55] contains 2000 videos with a total number of $14k$ clips. This dataset is collected from YouTube and covers 89 types of recipes. There are $\sim 9.6k$ clips for training and $\sim 3.2k$ clips for validation. For each clip, there is a manually annotated textual description.

Evaluation protocol. We evaluate the learned embeddings on the modality$-$to$-$modality retrieval task in terms of Recall@K, median rank (MdR), and mean rank (MnR). Given a query, its K nearest neighbours are retrieved from the database. The retrieval is considered successful, if the correct sample is among the K nearest neighbors.

4.2. Expert Features

We encode the content of a video with pre-trained models trained for different semantic tasks, namely appearance, scene, action, object, and howto100m [26]. We extract per-frame features. To be specific, we use a ResNeSt269 model [53] pretrained on ImageNet to extract appearance information, and a DenseNet161 model [54] pretrained on Places365 to extract scene information. In terms of action information, we adopt a R(2+1)D model [43] with ResNet152 backbone pretrained on IG65M, and extract the final global pooled feature. For object features, we use a Faster-RCNN model [35] with ResNet50 FPN backbone.

For Youcook2 experiments we use the Howto100m features provided by [12]. For LSMDC results in the Table 1, we used action and appearance features as input to the model. For the SOTA comparisons in Table 4 we utilized all expert features including appearance, action, scene, ob-

Table 1. **Comparison among contrastive learning losses.** Video-text retrieval results with different contrastive learning losses on the YouCook2 and LSMDC dataset. CrossCLR shows consistently higher retrieval scores than previous losses.

	Youcook2						LSMDC					
	Text $\implies$ Video			Video $\implies$ Text			Text $\implies$ Video			Video $\implies$ Text		
	R@1	R@5	R@10	R@1	R@5	R@10	R@1	R@5	R@10	R@1	R@5	R@10
MaxMargin [11, 24]	$15.0_{\pm 0.34}$	$37.0_{\pm 0.38}$	$49.1_{\pm 0.51}$	$14.2_{\pm 0.14}$	$35.3_{\pm 0.02}$	$47.2_{\pm 0.08}$	8.2	22.7	31.8	9.1	23.3	31.8
MIL-NCE [26]	$18.0_{\pm 0.23}$	$41.9_{\pm 0.53}$	$53.9_{\pm 1.06}$	$16.4_{\pm 0.51}$	$41.5_{\pm 0.24}$	$54.1_{\pm 0.54}$	8.9	24.2	32.5	10.4	25.4	34.9
CLIP [34]	$17.8_{\pm 0.40}$	$42.1_{\pm 0.78}$	$54.4_{\pm 0.66}$	$17.0_{\pm 0.54}$	$42.0_{\pm 0.48}$	$55.0_{\pm 0.58}$	9.7	24.1	32.6	9.5	23.8	32.5
DCL [7]	$17.9_{\pm 0.88}$	$41.5_{\pm 0.59}$	$54.1_{\pm 0.79}$	$16.8_{\pm 0.39}$	$42.0_{\pm 0.37}$	$55.3_{\pm 0.62}$	9.0	24.9	33.2	8.6	23.4	32.2
NT-Xent [4]	$17.5_{\pm 0.44}$	$42.4_{\pm 0.27}$	$55.0_{\pm 0.77}$	$17.3_{\pm 0.58}$	$41.6_{\pm 0.89}$	$54.6_{\pm 1.0}$	9.3	23.6	32.5	10.0	25.1	33.4
CrossCLR	$\mathbf{19.5_{\pm 0.49}}$	$\mathbf{45.9_{\pm 0.55}}$	$\mathbf{58.3_{\pm 0.76}}$	$\mathbf{18.5_{\pm 0.32}}$	$\mathbf{44.8_{\pm 0.82}}$	$\mathbf{57.9_{\pm 0.77}}$	**10.9**	**26.2**	**34.7**	**12.0**	**26.1**	**35.3**

Table 2. **Ablation study on CrossCLR loss.** We quantify the individual contributions of the CrossCLR components: proximity weighting (P_W), intra-modality alignment (I_M), and negative pruning (N_P) (reported avg and std over 5 runs).

P_W	I_M	N_P	Text $\implies$ Video			Video $\implies$ Text		
			R@1	R@5	R@10	R@1	R@5	R@10
✗	✗	✗	$17.9_{\pm 0.51}$	$41.7_{\pm 0.83}$	$53.7_{\pm 0.77}$	$16.7_{\pm 0.53}$	$40.9_{\pm 0.64}$	$53.7_{\pm 0.96}$
✓	✗	✗	$18.2_{\pm 0.39}$	$41.9_{\pm 1.28}$	$53.7_{\pm 1.12}$	$16.9_{\pm 1.18}$	$41.4_{\pm 1.04}$	$53.9_{\pm 1.33}$
✗	✓	✗	$18.7_{\pm 0.33}$	$43.6_{\pm 0.63}$	$56.2_{\pm 0.54}$	$17.7_{\pm 0.50}$	$42.8_{\pm 0.79}$	$56.3_{\pm 0.49}$
✓	✓	✗	$19.0_{\pm 0.42}$	$45.4_{\pm 0.98}$	$57.8_{\pm 0.97}$	$18.3_{\pm 0.35}$	$44.1_{\pm 1.13}$	$57.2_{\pm 1.11}$
✓	✓	✓	$\mathbf{19.5_{\pm 0.49}}$	$\mathbf{45.9_{\pm 0.55}}$	$\mathbf{58.3_{\pm 0.76}}$	$\mathbf{18.5_{\pm 0.32}}$	$\mathbf{44.8_{\pm 0.82}}$	$\mathbf{57.9_{\pm 0.77}}$

ject and howto100m features.

4.3. Implementation Details

We use the RADAM optimizer with momentum 0.56 and mini-batch size of 64. The initial learning rate is set to $7e4$. It is reduced by a factor of 10 when validation performance saturates. For each dataset, we use the corresponding validation set to estimate the hyperparameters. We use the following hyperparameters for the CrossCLR : $\kappa = 35e4$ for Youcook2 and $\kappa = 55e4$ for LSMDC
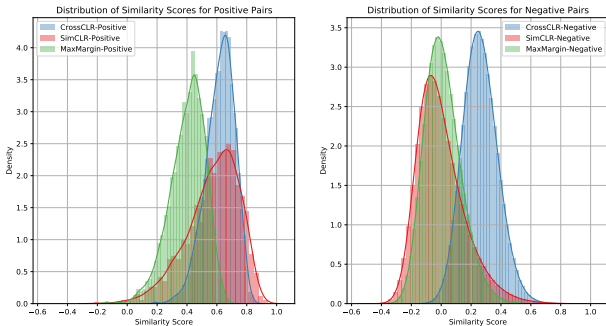

Figure 5. Distribution of similarity scores for positive pairs and negative pairs in the joint embedding after training for the Max-Margin, NT-Xent (SimCLR), and CrossCLR losses. CrossCLR yields a lower variance (more certainty) on positive pairs compared to MaxMargin and NT-Xent. For MaxMargin, also the mean is shifted towards smaller values, which means it has lower confidence in aligning similar semantics. For negative pairs, NT-Xent and MaxMargin's scores are concentrated around zero. In contrast, CrossCLR intrinsically considers similarity of negative pairs and therefore the concentration is shifted towards positive scores.

, $\lambda = 8e1$ for Youcook2 and $\lambda = 65e2$ for LSMDC, $\tau = 0.03$. We use threshold $\gamma = 0.9$ and queue size of $3K$ and $5K$ for Youcook2 and LSMDC datasets respectively. We train the models for 40 epochs which take ∼1 hour for Youcook2 and ∼2 hour for LSMDC datasets to train on one NVIDIA T4 Tensor core GPU. For further details on the architecture, we refer to the supplementary material.

4.4. Experiment Results

Ablation study of CrossCLR components. The proposed CrossCLR contains three components: the intra-modality alignment (I_M), proximity weighting (P_W), and negative pruning (N_P). To shed light on the contributions of these three components, we report the retrieval results on the Youcook2 dataset in Table 2. The data split and other experimental settings were kept identical. All three components have a positive impact on the results, individually and jointly. The intra-modality component I_M yields the largest individual gain, but also the concept of influential samples, as used by negative pruning and proximity weighting, yields a clear benefit.

Comparison to other contrastive learning methods. We compare the CrossCLR loss with popular contrastive losses: MaxMargin [46, 47, 11, 24], MILNCE [26], NT-Xent [3], CLIP [34], and DCL [7]. For the sake of a fair and direct comparison, we used the same experimental setup and architecture as COOT [12] and only exchanged the loss. Table 1 reports the retrieval performance on Youcook2 and LSMDC. CrossCLR consistently improves over previous contrastive learning methods on both datasets.

In Figure 5, we explore different contrastive learning methods, three contrastive methods SimCLR (NT-Xent), MaxMargin, and CrossCLR , w.r.t. their similarity scores of positive and negative pairs. We show the histograms of similarity scores for positive and negative samples separately. The scores are computed on the validation set after training the network with these three losses individually. Figure 5 reveals that CrossCLR yields a higher certainty (lower variance) for positive samples than the MaxMargin loss or SimCLR loss. The MaxMargin loss [46, 47, 11, 24] yields a significantly lower mean score for positive samples, which indicates that this method has issues installing
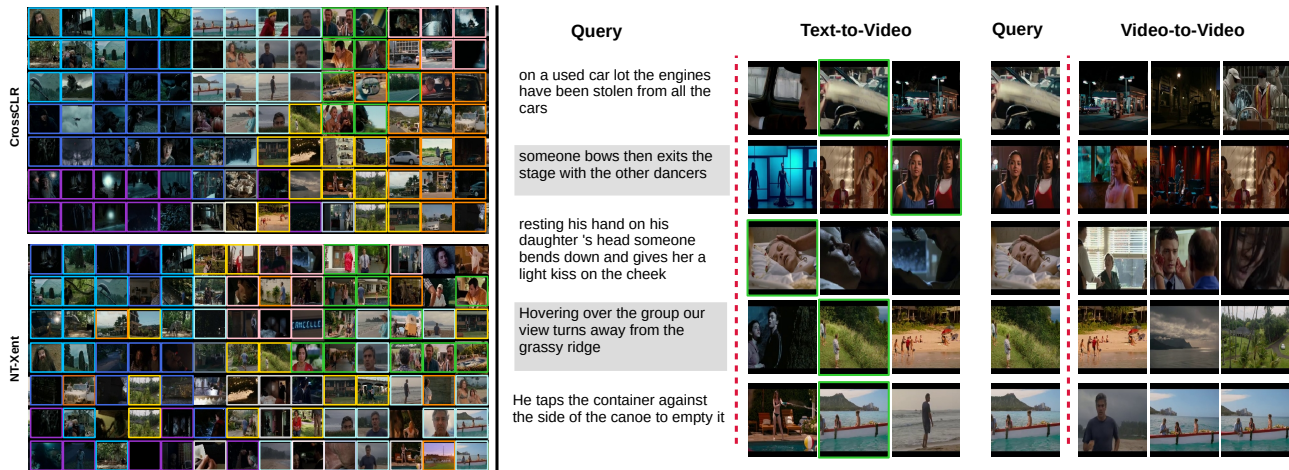
Figure 6. Qualitative results for LSMDC dataset (Best viewed in color). **Left**: We show the t-SNE visualization of embeddings for CrossCLR and NT-Xent based on text embeddings. Color of the boxes represent the similarity of semantics. CrossCLR has higher intra-modality consistency than NT-Xent. **Right**: It shows several examples for text-to-video (Top3 nearest neighbors) and video-to-video (Top3 nearest neighbors excluding self) retrieval task.

Table 3. **Comparison to the state-of-the-art text-to-video retrieval on Youcook2.** CrossCLR improves the state of the art (COOT) while using the same architecture and experimental settings.

	Text $\Longrightarrow$ Video		
	R@1	R@5	R@10
Random	0.03	0.15	0.3
Miech et al. [28]	6.1	17.3	24.8
ActBERT [57]	9.6	26.7	38.0
MIL-NCE [26]	15.1	38.0	51.2
COOT [12]	$16.7_{\pm 0.4}$	$40.2_{\pm 0.3}$	$52.3_{\pm 0.5}$
CrossCLR	$\mathbf{19.5}_{\pm 0.49}$	$\mathbf{45.9}_{\pm 0.55}$	$\mathbf{58.3}_{\pm 0.76}$

Table 4. **Comparison to the state-of-the-art text-to-video retrieval on LSMDC dataset (test split).** CrossCLR improves the state of the art (MMT).

	Text $\Longrightarrow$ Video				
	R@1	R@5	R@10	MdR$\downarrow$	MnR$\downarrow$
Random	0.1	0.5	1.0	500.0	500.0
CT-SAN [52]	5.1	16.3	25.2	46.0	–
JSFusion [51]	9.1	21.2	34.1	36.0	–
CCA [21]	7.5	21.7	31.0	33.0	–
MEE [27]	9.3	25.1	33.4	27.0	–
MEE-COCO [27]	10.1	25.6	34.6	27	–
CE [24]	11.2	26.9	34.8	25.3	–
MMT [11]	13.2	29.2	38.8	21.0	76.3
COOT [12]	11.3	26.1	36.7	22.0	85.4
CLIP [32]	11.3	22.7	29.2	56.5	–
CrossCLR	**15.0**	**32.5**	**42.0**	**18.0**	**74.4**

the provided training links between cross-modal concepts in the learned embedding. SimCLR [3] can represent more of these concepts, but the higher variance indicates that there are many failure cases, too. From the histograms over the negative sample scores we can see that SimCLR and MaxMargin loss both have zero mean for negative samples, as enforced by the structure of the loss. This does not allow for semantic overlap among negative samples. In contrast, CrossCLR allows for semantic similarity among negative samples, which shifts the distribution towards positive scores. This does not necessary mean that the relationships between negative samples enabled by CrossCLR are all meaningful. However, the improved retrieval performance after pruning of influential samples indirectly indicates that many of these relationships make sense.

Figure 6 shows gualitative visualization of learned embeddings. The qualitative samples in this figure show that CrossCLR brings more consistency over intra-modality samples in comparison to NT-Xent.

Comparison to the state of the art. Table 3 and Table 4 show that, thanks to the CrossCLR loss, retrieval performance from text to video improves over the state of the art on both the YouCook2 and the LSMDC dataset. For LSMDC experiment we utilized action, appearance, object, scene and howto100m features. However, MMT [11] utilizes additional modalities such as Audio, OCR and Face. CrossCLR outperforms MMT while using less modalities. Note that for LSMDC experiment in Table 4, we don't use sophisticated fusion techniques and just simply aggregate output of each model trained individually on each modality (more details in supplementary material). Since, we use the same architecture (Fig. 4) and experimental setup as COOT [12], with only the loss being different, the improvement can be directly attributed to CrossCLR .

Other pairs of modalities. We were interested whether the improvements obtained by CrossCLR are specific to video-text retrieval or if the loss generalizes well to other pairs of modalities. To this end, we compared CrossCLR to the NT-Xent loss [4] on various combinations of input modalities derived from the LSMDC dataset. Table 5 shows that, with very few exceptions, CrossCLR shows better retrieval performance than NT-Xent. This demon-

Table 5. **Generalization to other pairs of modalities.** Modality-to-modality retrieval on the full grid of modalities for the LSMDC dataset. CrossCLR yields improved retrieval scores for almost all pairs of modalities.

Modality	Method	Text		Appearance		Object		Scene		Action		**Mean**	
		R@1	R@10	R@1	R@10	R@1	R@10	R@1	R@10	R@1	R@10	R@1	R@10
Text	NT-Xent	— —	— —	7.2	28.3	2.8	8.3	5.7	24.7	9.3	32.6	6.3	23.5
	CrossCLR	— —	— —	8.1	29.3	2.5	9.6	7.4	25.3	10.2	33.3	**7.1**	**24.4**
Appearance	NT-Xent	7.1	27.5	— —	— —	72.7	92.2	98.3	100	85.6	98.2	65.9	79.5
	CrossCLR	8.8	30.0	— —	— —	75.8	93.8	99.5	100	85.4	98.9	**67.4**	**80.7**
Object	NT-Xent	2.4	8.3	68.6	91.5	— —	— —	75.4	95.2	43.2	80.5	47.4	68.9
	CrossCLR	3.1	9.0	74.7	94.7	— —	— —	79.5	95.9	43.3	82.4	**50.2**	**70.5**
Scene	NT-Xent	6.2	24.3	98.5	100	82.8	95.6	— —	— —	86.8	98.7	**68.6**	79.7
	CrossCLR	7.4	25.0	99.6	100	84.0	96.0	— —	— —	83.0	98.8	68.5	**80.0**
Action	NT-Xent	7.6	31.7	84.8	97.9	47.1	85.4	85.3	98.5	— —	— —	56.2	78.4
	CrossCLR	9.7	33.0	85.0	98.8	50.3	86.2	86.1	98.7	— —	— —	**57.8**	**79.2**
Mean	NT-Xent	5.8	23.0	64.8	79.4	51.4	70.4	66.2	79.6	**56.2**	77.5	— —	— —
	CrossCLR	**7.3**	**24.3**	**66.9**	**80.7**	**53.2**	**71.4**	**68.1**	**80.0**	55.5	**78.4**	— —	— —

Table 6. **Captioning performance on the YouCook2 dataset.** We follow the setup from COOT [12] and report captioning results on the validation split, given ground truth video segments. The last row shows the human performance and can be considered as the best achievable performance as reported by Hessel et al [17]. $^+$ We use video embeddings in addition to clip embeddings as input to model. * Vedantam et al. [45] introduced two versions CIDEr and CIDEr-D. We report CIDEr-D [45], however for methods with * sign we couldn't find the information about the version they used.

Method	B@3	B@4	RougeL	METEOR	CIDEr-D	RE@4↓
VideoBERT [42]	7.59	4.33	28.80	11.94	—*	—
ActBERT [57]	8.66	5.41	30.56	13.30	—*	—
Zhou et al. [56]	7.53	3.84	27.44	11.55	—*	—
VTransformer [56]	13.08	7.62	32.18	15.65	32.26	7.83
TransformerXL [8]	11.46	6.56	30.78	14.76	26.35	6.30
MART [22]	12.83	8.00	31.97	15.90	35.74	4.39
AT+Video [17]	—	9.01	36.65	17.77	—*	—
COOT [12]	17.12	10.91	37.59	18.85	54.07	5.11
CrossCLR	17.60	11.11	38.00	19.25	58.65	**4.19**
COOT [12]$^+$	17.97	11.30	37.94	19.85	57.24	6.69
CrossCLR$^+$	**18.62**	**12.04**	**38.63**	**20.17**	**61.10**	5.62
Human [17]	—	15.20	45.10	25.90	—	—

strates that the principles behind CrossCLR are not specific to video-text retrieval but are applicable to learning cross-modal embeddings in general.

4.5. Video Captioning

In addition to the video-text retrieval, we report the captioning performance to show the richness of learned embeddings with CrossCLR. Table 6 reports the captioning performance of learned embeddings with CrossCLR method in comparison to state-of-the-art methods on Youcook2 validation set.

We evaluate the captioning performance similar to MART [22] and COOT [12] with the metrics CIDEr-D [45], ROUGE-L [23], BLEU@3 and BLEU@4 [31], and METEOR [9]. Additionaly, we utilize repetition metric RE@4 [50] to measure the reptition of the caption. We feed the clip embeddings generated with our CrossCLR method to the captioning model MART [22] (additionally

we also use video embeddings for $^+$ experiment). In comparison to COOT we obtain more diverse and accurate captions. MART [22] uses appearance and optical flow features extracted from ResNet-200 and BN-Inception models, respectively. According to all metrics, CrossCLR outperforms state-of-the-art significantly and also generates more diverse captions compared to other methods.

5. Conclusion

We introduced a contrastive loss for learning joint embeddings of two input modalities that respects the special need of cross-modal learning. First, assuming that the input modalities already come with some meaningful embedding where semantically related concepts are close in feature space, we enforced this proximity also in the joint embedding. Previous losses did not use this constraint, partially because they primarily focus on learning feature representations of the input modalities from scratch rather than learning a joint embedding. In our experiments, the intra-modal proximity led to consistent benefits in cross-modal retrieval performance. Second, we identified the problem of false negative samples and proposed a heuristic to identify false negatives via the degree of interconnections in the input embedding. Also this, together with the proximity weighting, led to consistent improvements in retrieval performance. Finally, we showed that the improvements obtained with CrossCLR are not limited to video and text embeddings. The same principle can be successfully applied to other pairs of modalities to learn joint embeddings.
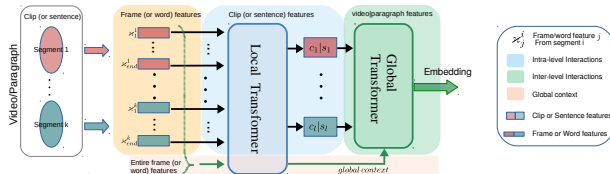
Figure 7. **Overview of architecture** (best viewed in color). We use the same architecture as COOT [12] which consist of two branches: one for video input and one for text input. Since both streams have same design, we here only show one branch. After encoding video data and it's corresponding text, we fed them to local transformer to obtain clip/sentence level features. Then, global transformer aggregates the clip/sentence level features and produces video/paragraph features. The CrossCLR loss is applied to both local (clip/sentence) and global (video/paragraph) features.

Appendices

A. Architecture

A video v_i is represented as a collection of consecutive clips $vi = [c_{i1}, c_{i2}, \ldots, c_{il}]$, and similarly we define paragraph p_i as a list of sentences $p_i = [s_{i1}, s_{i2}, \ldots, s_{il}]$. Each pair video v_i and paragraph p_i and also their clips (c_{ij}) and sentences (s_{ij}) are considered temporally aligned.

We first apply pre-trained visual encoders (appearance, object, etc) to extract per-frame features, where a clip c_{ij} contains t frames. For the sentence s_{ij} with h words, we utilize *Bert-Based uncased* model to extract features. As explained in Section 4.3, for Youcook2 we use HowTo100m pre-trained model [12] to encode video frames.

Note that our architecture is same as COOT. However, We remove all losses used in COOT and only apply Cross-CLR in two points. In the architecture 7, we apply Cross-CLR in two locations: clip and sentence features obtained after local transformer; video and paragraph features obtained after global transformer. In all experiments, we train the model with the following objective: $L_{local} + 0.6 L_{global}$. For L_{local} we use CrossCLR with queue (hyper-parameters in Table 7) and for L_{global} we use the CrossCLR without queue. Pseudo-code of CrossCLR without queue in Algorithm 2 is shown in PyTorch style.

B. Hyper-parameters

We list the hyper-parameters and ranges used during training. We largely follow prior work [12] for architecture hyper-parameters and for the rest we tuned hyper-parameters based on the performance on validation set. In general, we found retrieval performance to increase with larger queue capacity. In Table 7, we report the hyper-parameters used in the experiments.

Table 7. **Hyperparameters.** This table shows the hyperparameter ranges we considered and the final choices for LSMDC and YouCook2 datasets. First block shows the hyperparameters for optimizer, second block provides the architecture setting and last block shows the hyperparameters for our CrossCLR loss. AF is our Attention-aware Feature Aggregation module.

Hyperparameter	Range	LSMDC	Youcook2
Optimizer	RAdam	RAdam	RAdam
Learning rate	5e-5 - 1e-3	7e-4	7e-4
Weight Decay	0	0	0
Momentum	0.56	0.56	0.56
Warmup Epochs	4	4	4
Reduce on Plateau-Patience	6	6	6
Reduce on Plateau-Cooldown	4	4	4
Attention Layers	1	1	1
Attention Dimension	[384, 768]	768	384
Attention Heads-Local	[4, 8, 16]	16	8
Attention Heads-Global	1 - 8	8	8
AF Heads	[4, 8]	-	2
Pooler	[Max, ATN]	Max	ATN
Dropout	1% - 10%	1%	5%
Temperature τ	0.03	0.03	0.03
Weight scale κ	1e-5 - 1	55e-4	35e-4
Intra-modality weight λ	0.1-1	65e-1	8e-1
Pruning threshold γ	0.1-1	0.9	0.9
Queue size	1,000-10,000	3,000	5,000

B.1. Effect of Pruning Threshold

Figure 10, presents a graph visualization of the Youcook2 dataset embeddings. As can be seen, some samples have dense connections to other samples which means those samples are semantically similar to many samples. Therefore, it's critical to remove these highly similar samples from the negative set to prevent semantic collision, as discussed in section 3.2 of paper. We change the pruning threshold from $1e1$ to 1 and show the results in Figure 8. To prune samples from the negative set, we first divide all scores in each set by the maximum score and then remove the samples which have score above the threshold. Therefore, increasing threshold means removing samples with higher similarity but keeping the other samples which have scores less than threshold. We consider thresholds $\gamma \in \{0.1, 0.2, 0.3, 0.4, 0.5, 0.6, 0.7, 0.8, 0.9, 1\}$ and $\gamma = 1$ means no pruning. As shown in Figure 8, increasing the threshold results in higher performance until $\gamma = 0.9$ and after that again performance decreases. We found that for both LSMDC and Youcook2 datasets $\gamma = 0.9$ is a reasonable number.

B.2. Effect of Weight Scale

Figure 9, shows the retrieval performance with different κ values. We train three models for each $\kappa \in \{0.1, 0.01, 0.001, 0.003, 0.005, 0.007, 0.009\}$. When weight scale is too high, CrossCLR does not converge very well. But with numbers around 0.003-0.005 model performs very well.
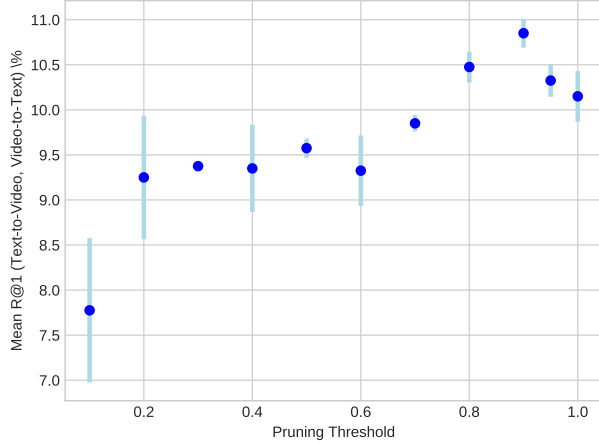
Figure 8. **Impact of Pruning Threshold**. We evaluate the effect of pruning threshold on the retrieval performance for LSMDC dataset using appearnce and action features.
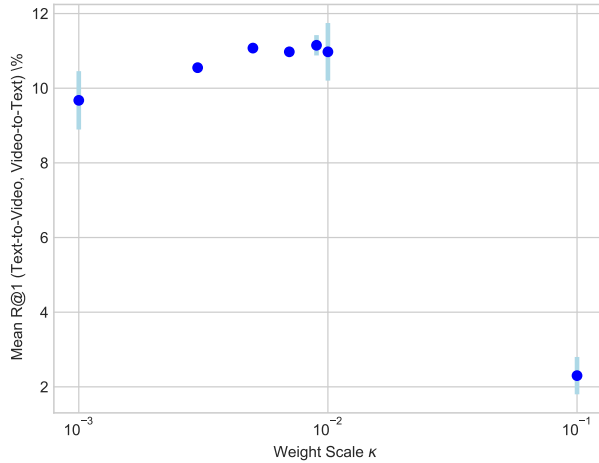

Figure 9. **Impact of Weight Scale** κ. CrossCLR is stable against small changes in κ.

C. Experiments

C.1. Do multiple positives in CrossCLR help?

In this section, we empirically asses the effect of having multiple positives in objective function. We define our CrossCLR loss with multiple positive samples as following:

$$L_x = -\mathbb{E}_{i\in\mathcal{M}} \left[w(x_i) \log \frac{\delta(x_i,y_i)+\beta \sum\limits_{y_k\in P_y} \delta(x_i,y_k)}{\delta(x_i,y_i)+\sum\limits_{y_k\in \dot{N}_x^E} \delta(x_i,y_k)+\lambda \sum\limits_{x_k\in \dot{N}_x^R} \delta(x_i,x_k)} \right] \quad (8)$$

$$L_y = -\mathbb{E}_{i\in\mathcal{M}} \left[w(y_i) \log \frac{\delta(y_i,x_i)+\beta \sum\limits_{x_k\in P_x} \delta(y_i,x_k)}{\delta(y_i,x_i)+\sum\limits_{x_k\in \dot{N}_y^E} \delta(y_i,x_k)+\lambda \sum\limits_{y_k\in \dot{N}_y^R} \delta(y_i,y_k)} \right] \quad (9)$$

Where β is a scaling factor for extra postive samples, P_x and P_y are positive samples for L_x and L_y respectfully. To construct the positive set, we select the top-K similar
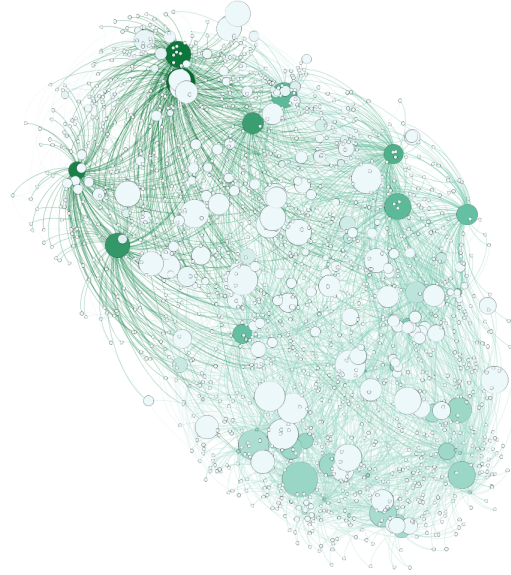

Figure 10. Graph representation of connections among samples in Youcook2 dataset. Each sample is connected to another sample if their feature similarity is above a certain threshold. Influential samples are densely connected to other samples and therefore share similar features with many other samples.

samples to the pivot sample among the influential samples. To be precise, $P_x = \{x_k | k \in topK(\mathcal{I}_y)\}$ and $P_y = \{y_k | k \in topK(\mathcal{I}_x)\}$. The results are shown in Table 8. In this experiment, for Youcook2 dataset we found that using $K = 2$ and $\beta = 0.15$ works best. For LSMDC dataset, we used $K = 5$ and $\beta = 0.2$. CrossCLR+MP on Youcook2 performs similar to the CrossCLR without multiple positives. However, on LSMDC we observe improvement when multiple positives are used. LSMDC dataset is larger than Youcook2 dataset and therefore it's easier to find very close positive samples to the original sample. Note that, removing influential samples from the negative set reduces the effect of pushing away samples with common semantics. But for multiple positives case, optimization tries to align positive samples and therefore it requires samples to be semantically very close otherwise alignment is wrong.

C.2. Impact of different modality combinations:

We study the importance of different modality experts and their combinations on representation learning in Table 9. Using stronger features result in higher performance. The object expert modality gives the lowest performance and action modality produces the best performance in single modality setting. Additionally, we compare the retrieval performance with different combinations of modalities. To combine several modalities, we simply concatenate the features. In addtion, we also trained the network with combining two modalities and inputing them

Table 8. **Effect of Multiple Positives in CrossCLR Loss.** Comparison between our CrossCLR with multiple positives (MP) and standard CrossCLR which does not have multiple positives. For LSMDC experiment, we use appearance and action features together.

	Youcook2						LSMDC					
	Text $\implies$ Video			Video $\implies$ Text			Text $\implies$ Video			Video $\implies$ Text		
	R@1	R@5	R@10	R@1	R@5	R@10	R@1	R@5	R@10	R@1	R@5	R@10
CrossCLR	$19.5_{\pm0.49}$	$45.9_{\pm0.55}$	$58.3_{\pm0.76}$	$18.5_{\pm0.32}$	$44.8_{\pm0.82}$	$57.9_{\pm0.77}$	10.9	26.2	34.7	12.0	26.1	35.3
CrossCLR+MP	$19.3_{\pm0.51}$	$45.3_{\pm0.85}$	$58.2_{\pm0.77}$	$18.4_{\pm0.45}$	$44.4_{\pm0.61}$	$57.6_{\pm0.81}$	11.2	26.6	35.8	12.9	27.4	36.4

Table 9. **Performance of different modality combinations.** + We feed both modalities to network. ⊕ we train the network on each modality separately and then output embeddings are concatenated.

	Text $\implies$ Video				
	R@1	R@5	R@10	MdR↓	MnR↓
Random	0.1	0.5	1.0	500.0	500.0
Object	2.1	7.7	14.3	108.0	187.3
Scene	5.9	18.2	24.9	57.0	132.4
HowTo100M	6.4	18.9	26.4	44.0	115.0
Appearance	9.1	22.8	32.0	41.0	120.4
Action	9.3	22.3	30.7	36.0	112.3
Action+Scene	8.8	25.9	34.3	25.0	88.8
Action+HowTo100M	9.6	24.1	35.1	26.0	86.7
Action+Object	9.7	23.9	31.7	31.0	102.8
Action+Appearance	10.9	26.2	34.7	27.0	91.0
Scene ⊕ Object	6.0	17.8	24.8	55.0	130.6
HowTo100M ⊕ Object	6.4	19.4	27.3	44.0	114.8
Appearance ⊕ Object	8.2	22.7	29.4	44.0	121.1
Scene ⊕ HowTo100M	8.7	23.6	30.1	37.0	102.7
Action ⊕ Object	9.0	23.1	31.4	35.0	109.3
Action ⊕ HowTo100M	10.1	26.3	36.0	24.0	90.4
Scene ⊕ Appearance	10.2	24.2	32.0	39.0	111.0
HowTo100M ⊕ Appearance	10.5	25.5	34.4	31.0	97.3
Action ⊕ Scene	11.0	24.9	34.3	30.0	96.9
Action ⊕ Appearance	12.0	27.7	36.2	24.0	92.4
Scene ⊕ Object ⊕ HowTo100M	8.0	22.4	30.8	37.0	106.0
Object ⊕ Appearance ⊕ HowTo100M	9.4	26.5	34.1	34.0	101.1
Scene ⊕ Appearance ⊕ Object	9.2	23.3	31.9	38.0	112.4
Action ⊕ Scene ⊕ Object	10.0	25.2	33.6	32.0	100.1
Scene ⊕ Appearance ⊕ HowTo100M	10.8	26.8	34.4	32.0	97.3
Action ⊕ HowTo100M ⊕ Object	11.3	26.4	34.2	27.0	93.1
Action ⊕ Scene ⊕ HowTo100M	11.8	27.2	36.5	23.0	88.2
Action ⊕ Appearance ⊕ Object	12.4	27.5	35.7	28.0	95.7
Action ⊕ Appearance ⊕ Scene	12.6	27.2	36.7	24.0	91.5
Action ⊕ Appearance ⊕ HowTo100M	13.4	28.4	37.8	22.0	84.9

to network (Table 9 second block from top shown with +). In this paper, we don't study the architecture design for combining multiple modalities and therefore leave this question for future studies.

Challenges with Object Features: In Table 9, the object features provide lower performance in comparison to scene or action experts. The reason is that current object detection models are not trained on real-world or large scale movie datasets. Therefore these models cannot detect objects very well due to domain shift or high variations in visual features and high number of objects. In our experiments, we used a Faster RCNN [35] model and used all objects detected with score above 0.7. In Figure 11, we visualized some of challenging cases in object detection.

D. Qualitative Results

Figure 12, shows two qualitative examples for video captioning on Youcook2 dataset (samples are selected randomly for a fair comparison with COOT and MART). In

Figure 11. **Challenges in Object Detection for Movie Videos.** We show several qualitative examples of failure in object detection. **No labeling**: model cannot detect any object in the frame while there is an object, **Over labeling:** Labeling same object several times, **Wrong labeling:** Wrong category for the detected object, and **Unknown objects:** Since some objects are not labeled (or doesn't exist) in the training set of object detection model, these objects that cannot be recognized by the model.

MART: Add tomatoes and beef to a pot. Add water to the pan. Add tomato puree and salt. Add the beef and parsley to the soup. Add the beef to the pot. Add water to the soup and let it simmer. Add the soup to the soup.

COOT: Add the tomatoes and onions to a food processor and blend them. Add the tomatoes and a bay leaf to the pot. Add the tomatoes and simmer. Remove the tomatoes from the pot and let it cook. Remove the tomatoes from the pot and let it cook. Strain the soup to a boil and let it boil. Turn on the heat and heat to a boil.

CrossCLR: Add chopped tomatoes and onions to a pot. Add water to the pan. Add the tomatoes and cover to cook for 5 minutes. Drain the tomatoes and let the liquid cool. Add chopped tomatoes to the pot and simmer. Strain the tomato mixture to a blender and blend the soup. Heat the pot on a stove and let it boil.

GT: Add tomato onion green chili and rice to a pan. Add water to the pan. Boil the ingredients and then turn down the heat. Strain the ingredients. Blend the ingredients. Add the water to the mixture and strain. Boil the soup.

MART: Add flour to a bowl and whisk. Cut the chicken into pieces. Coat the chicken in flour. Coat the chicken in flour egg and breadcrumbs. Fry the chicken in a pan. Drizzle the sauce on top of the bread. Add sauce to the pizza. Bake the dish in the oven.

COOT: Mix parmesan cheese black pepper and garlic powder. Cover the chicken in the bag. Coat the chicken in the flour. Coat the chicken in the egg and coat with flour. Place the chicken in a pan and fry it on a pan. Pour sauce on top of the chicken and top with mozzarella cheese. Sprinkle parmesan cheese on top. Bake the chicken in the oven.

CrossCLR: Mix flour salt pepper and cayenne pepper. Pound the chicken. Coat the chicken in the egg. Coat the chicken in the egg and bread crumbs. Fry the chicken in a pan. Spread tomato sauce and mozzarella cheese on the chicken. Sprinkle cheese on top. Bake the dish in the oven.

GT: Mix bread crumbs and parmesan cheese. Pound the chicken. Rub salt and pepper onto the chicken. Rub flour onto the chicken dip it in egg and coat with breadcrumbs. Fry the chicken in a pan. Spread sauce over the chicken. Top the chicken with mozzarella cheese. Bake the chicken in the oven.

Figure 12. **Captioning samples for Youcook2 dataset**. We randomly selected two samples for video captioning to have a fair comparison with COOT and MART methods. Green: correct captioning, Yellow: Ok but not accurate, and Red: wrong captioning.

Figure 13, we visualize the video frames in the embed-

Algorithm 2 Pseudocode of CrossCLR (no queue version) in a PyTorch style.

bmm: batch matrix multiplication; mm: matrix multiplication; cat: concatenation.

```python
# enc_v, enc_t: encoder networks for video and
    text
# in_v, in_t: input video and text embeddings (BxD
    )
# B: batch size
# t: temperature, n_keep: 1-(pruning_percentage)
# t_w: loss weightening temperature
# mask = 1-np.eye(B)
# def norm_w(x): return x/sum(x)
# def mean_w(x,w,t): return sum(x)/(sum(exp(w/t)))

# Encode input video and text embeddings
emb_v, emb_t = enc_v(in_v), enc_t(in_t)

# Compute positive and negative logits
l_vt = mm(emb_v,emb_t.t())/t #video to text
l_tv = mm(emb_t,emb_v.t())/t #text to video
l_vv = (mm(emb_v,emb_v.t())/t)*mask #video to
    video
l_tt = (mm(emb_t,emb_t.t())/t)*mask #text to text

# Compute proximity of semantics
prox_vid = mean(mm(in_v, in_v.t()) * mask)
prox_txt = mean(mm(in_t, in_t.t()) * mask)
scores_v = prox_vid / max(prox_vid)
scores_t = prox_txt / max(prox_txt)

# Prune samples from intra-modality negative set
l_vv_p = l_vv[:, scores_v<threshold]
l_tt_p = l_tt[:, scores_t<threshold]

# Prune samples from inter-modality negative set
l_vt_p = l_vt[:, scores_v<threshold]
l_tv_p = l_tv[:, scores_t<threshold]

# Concatenate positive and negative logits
l_vtv = cat([l_vt_p, t_w * l_vv_p], dim=1)
l_tvt = cat([l_tv_p, t_w * l_tt_p], dim=1)

# compute the loss. Crossentropy without reduction
labels = arange(l_vt.shape[0])
loss_vtv = cross_entropy_loss(l_vtv, labels)
loss_tvt = cross_entropy_loss(l_tvt, labels)

# Weight losses based on semantic proximity
w_vtv = norm_w(prox_vid)
w_tvt = norm_w(prox_vid)
loss_vtv = loss_vtv * exp(w_vtv / t_w)
loss_tvt = loss_tvt * exp(w_tvt / t_w)

loss = (mean_w(loss_vtv, w_vtv, t_w) +
        mean_w(loss_tvt, w_tvt, t_w) ) /2
```

ding space based on distances between text embeddings for Youcook2 dataset. Two videos are close to each other if their text features are similar to each other. We use t-SNE and project the text embeddings to 2D space and then visualize each point with it's corresponding video frame. As can be seen, the text embeddings are clustered semantically and aligned with visual semantics.

References

[1] Sanjeev Arora, Hrishikesh Khandeparkar, Mikhail Khodak, Orestis Plevrakis, and Nikunj Saunshi. A theoretical analysis of contrastive unsupervised representation learning, 2019. 4

[2] Mathilde Caron, Ishan Misra, Julien Mairal, Priya Goyal, Piotr Bojanowski, and Armand Joulin. Unsupervised Learning of Visual Features by Contrasting Cluster Assignments. *arXiv preprint arXiv:2006.09882*, 2020. 2
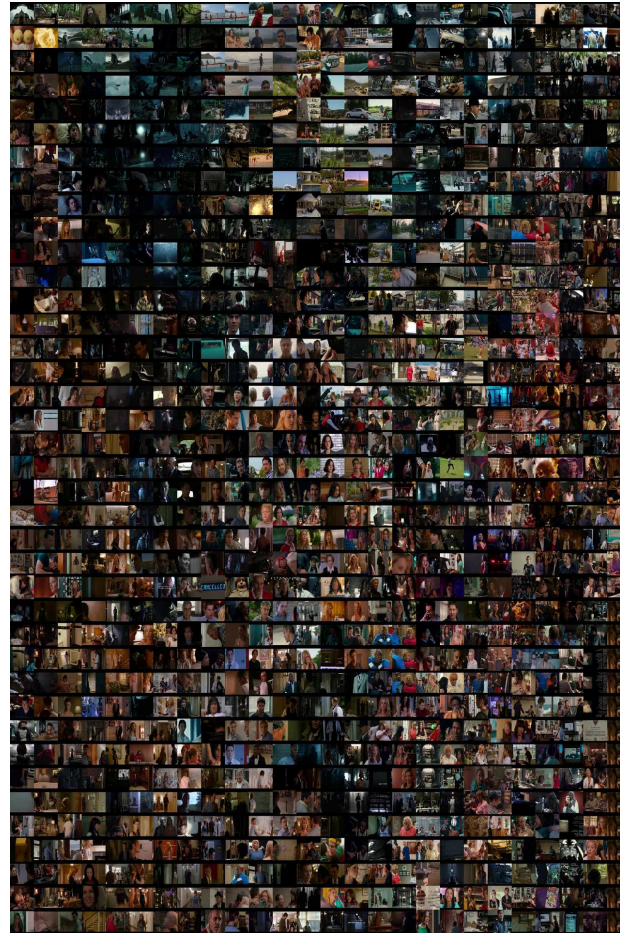
Figure 13. **Visualization of the video frames based on their text embeddings**. We use t-SNE to project text embeddings to 2D space and then present each point with it's corresponding video frame.

[3] Ting Chen, Simon Kornblith, Mohammad Norouzi, and Geoffrey Hinton. A Simple Framework for Contrastive Learning of Visual Representations. In *ICML*. 2020. 1, 2, 6, 7

[4] Ting Chen, Simon Kornblith, Mohammad Norouzi, and Geoffrey Hinton. A simple framework for contrastive learning of visual representations. In *International conference on machine learning*, pages 1597–1607. PMLR, 2020. 6, 7

[5] Ting Chen, Simon Kornblith, Kevin Swersky, Mohammad Norouzi, and Geoffrey Hinton. Big Self-Supervised Models are Strong Semi-Supervised Learners. *arXiv preprint arXiv:2006.10029*, 2020. 2

[6] Xinlei Chen, Haoqi Fan, Ross Girshick, and Kaiming He. Improved baselines with momentum contrastive learning. *arXiv preprint arXiv:2003.04297*, 2020. 2, 4

[7] Ching-Yao Chuang, Joshua Robinson, Yen-Chen Lin, Antonio Torralba, and Stefanie Jegelka. Debiased contrastive learning. *Advances in Neural Information Processing Systems*, 33, 2020. 4, 6

[8] Zihang Dai, Zhilin Yang, Yiming Yang, Jaime Carbonell, Quoc V. Le, and Ruslan Salakhutdinov. Transformer-xl:

Attentive language models beyond a fixed-length context, 2019. 8

[9] Michael Denkowski and Alon Lavie. Meteor universal: Language specific translation evaluation for any target language. In *Proceedings of the Ninth Workshop on Statistical Machine Translation*, pages 376–380, Baltimore, Maryland, USA, Jun 2014. Association for Computational Linguistics. 8

[10] Jianfeng Dong, Xirong Li, Chaoxi Xu, Shouling Ji, Yuan He, Gang Yang, and Xun Wang. Dual encoding for zero-example video retrieval. In *IEEE Conference on Computer Vision and Pattern Recognition, CVPR 2019, Long Beach, CA, USA, June 16-20, 2019*, pages 9346–9355. Computer Vision Foundation / IEEE, 2019. 1

[11] Valentin Gabeur, Chen Sun, Karteek Alahari, and Cordelia Schmid. Multi-modal transformer for video retrieval, 2020. 1, 2, 3, 6, 7

[12] Simon Ging, Mohammadreza Zolfaghari, Hamed Pirsiavash, and Thomas Brox. Coot: Cooperative hierarchical transformer for video-text representation learning. In *Advances on Neural Information Processing Systems (NeurIPS)*, 2020. 1, 2, 3, 5, 6, 7, 8, 9

[13] Jean-Bastien Grill, Florian Strub, Florent Altché, Corentin Tallec, Pierre H. Richemond, Elena Buchatskaya, Carl Doersch, Bernardo Avila Pires, Zhaohan Daniel Guo, Mohammad Gheshlaghi Azar, Bilal Piot, Koray Kavukcuoglu, Rémi Munos, and Michal Valko. Bootstrap Your Own Latent: A New Approach to Self-Supervised Learning. *arXiv preprint arXiv:2006.07733*, 2020. 2

[14] R. Hadsell, S. Chopra, and Y. LeCun. Dimensionality reduction by learning an invariant mapping. In *2006 IEEE Computer Society Conference on Computer Vision and Pattern Recognition (CVPR'06)*, volume 2, pages 1735–1742, 2006. 1

[15] Tengda Han, Weidi Xie, and Andrew Zisserman. Self-supervised co-training for video representation learning. In *Neurips*, 2020. 2

[16] Kaiming He, Haoqi Fan, Yuxin Wu, Saining Xie, and Ross Girshick. Momentum Contrast for Unsupervised Visual Representation Learning. In *CVPR*. 2020. 2, 4

[17] Jack Hessel, Bo Pang, Zhenhai Zhu, and Radu Soricut. A case study on combining ASR and visual features for generating instructional video captions. *CoRR*, abs/1910.02930, 2019. 8

[18] Elad Hoffer and Nir Ailon. Deep metric learning using triplet network. In Aasa Feragen, Marcello Pelillo, and Marco Loog, editors, *Similarity-Based Pattern Recognition - Third International Workshop, SIMBAD 2015, Copenhagen, Denmark, October 12-14, 2015, Proceedings*, volume 9370 of *Lecture Notes in Computer Science*, pages 84–92. Springer, 2015. 1

[19] Yannis Kalantidis, Mert Bulent Sariyildiz, Noe Pion, Philippe Weinzaepfel, and Diane Larlus. Hard Negative Mixing for Contrastive Learning. *NeurIPS*, 2020. 2

[20] Prannay Khosla, Piotr Teterwak, Chen Wang, Aaron Sarna, Yonglong Tian, Phillip Isola, Aaron Maschinot, Ce Liu, and Dilip Krishnan. Supervised contrastive learning. *arXiv preprint arXiv:2004.11362*, 2020. 2

[21] Benjamin Klein, Guy Lev, Gil Sadeh, and Lior Wolf. Associating neural word embeddings with deep image representations using fisher vectors. In *Proceedings of the IEEE Conference on Computer Vision and Pattern Recognition*, pages 4437–4446, 2015. 7

[22] Jie Lei, Liwei Wang, Yelong Shen, Dong Yu, Tamara L Berg, and Mohit Bansal. Mart: Memory-augmented recurrent transformer for coherent video paragraph captioning. In *ACL*, 2020. 8

[23] Chin-Yew Lin. Rouge: A package for automatic evaluation of summaries. In *Text Summarization Branches Out*, pages 74–81, Barcelona, Spain, Jul 2004. Association for Computational Linguistics. 8

[24] Yang Liu, Samuel Albanie, Arsha Nagrani, and Andrew Zisserman. Use what you have: Video retrieval using representations from collaborative experts. In *30th British Machine Vision Conference 2019, BMVC 2019, Cardiff, UK, September 9-12, 2019*, page 279. BMVA Press, 2019. 1, 2, 3, 6, 7

[25] Shuang Ma, Zhaoyang Zeng, Daniel McDuff, and Yale Song. Learning audio-visual representations with active contrastive coding, 2020. 1

[26] Antoine Miech, Jean-Baptiste Alayrac, Lucas Smaira, Ivan Laptev, Josef Sivic, and Andrew Zisserman. End-to-End Learning of Visual Representations from Uncurated Instructional Videos. In *CVPR*, 2020. 1, 2, 5, 6, 7

[27] Antoine Miech, Ivan Laptev, and Josef Sivic. Learning a text-video embedding from incomplete and heterogeneous data. *arXiv preprint arXiv:1804.02516*, 2018. 2, 3, 7

[28] Antoine Miech, Dimitri Zhukov, Jean-Baptiste Alayrac, Makarand Tapaswi, Ivan Laptev, and Josef Sivic. HowTo100M: Learning a Text-Video Embedding by Watching Hundred Million Narrated Video Clips. In *ICCV*, 2019. 1, 2, 7

[29] Niluthpol C Mithun, Juncheng Li, Florian Metze, and Amit K Roy-Chowdhury. Learning joint embedding with multimodal cues for cross-modal video-text retrieval. In *ICMR*. ACM, 2018. 3

[30] Pedro Morgado, Yi Li, and Nuno Vasconcelos. Learning representations from audio-visual spatial alignment, 2020. 1

[31] Kishore Papineni, Salim Roukos, Todd Ward, and Wei-Jing Zhu. Bleu: a method for automatic evaluation of machine translation. In *Proceedings of the 40th Annual Meeting of the Association for Computational Linguistics*, pages 311–318, Philadelphia, Pennsylvania, USA, Jul 2002. Association for Computational Linguistics. 8

[32] Jesús Andrés Portillo-Quintero, José Carlos Ortiz-Bayliss, and Hugo Terashima-Marín. A straightforward framework for video retrieval using clip, 2021. 7

[33] Rui Qian, Tianjian Meng, Boqing Gong, Ming-Hsuan Yang, Huisheng Wang, Serge J. Belongie, and Yin Cui. Spatiotemporal contrastive video representation learning. *CoRR*, abs/2008.03800, 2020. 1

[34] Alec Radford, Jong Wook Kim, Chris Hallacy, Aditya Ramesh, Gabriel Goh, Sandhini Agarwal, Girish Sastry, Amanda Askell, Pamela Mishkin, Jack Clark, et al. Learning transferable visual models from natural language supervision. *Image*, 2:T2, 2021. 1, 2, 4, 6

[35] Shaoqing Ren, Kaiming He, Ross Girshick, and Jian Sun. Faster r-cnn: Towards real-time object detection with region proposal networks, 2016. 5, 11

[36] Joshua Robinson, Ching-Yao Chuang, Suvrit Sra, and Stefanie Jegelka. Contrastive Learning with Hard Negative Samples. *ICLR*, 2021. 2

[37] A. Rohrbach, M. Rohrbach, N. Tandon, and B. Schiele. A dataset for movie description. In *2015 IEEE Conference on Computer Vision and Pattern Recognition (CVPR)*, pages 3202–3212, 2015. 5

[38] Xiaokang Yang Shaofeng Zhang, Junchi Yan. Self-supervised representation learning via adaptive hard-positive mining. *https://openreview.net/forum?id=aLIbnLY9NtH*, 2020. 2

[39] Kihyuk Sohn, Chun-Liang Li, Jinsung Yoon, Minho Jin, and Tomas Pfister. Learning and evaluating representations for deep one-class classification, 2020. 4

[40] Y. Suh, B. Han, W. Kim, and K. M. Lee. Stochastic class-based hard example mining for deep metric learning. In *2019 IEEE/CVF Conference on Computer Vision and Pattern Recognition (CVPR)*, pages 7244–7252, 2019. 4

[41] C. Sun, A. Myers, C. Vondrick, K. Murphy, and C. Schmid. Videobert: A joint model for video and language representation learning. In *2019 IEEE/CVF International Conference on Computer Vision (ICCV)*, pages 7463–7472, 2019. 1, 2

[42] Chen Sun, Austin Myers, Carl Vondrick, Kevin Murphy, and Cordelia Schmid. Videobert: A joint model for video and language representation learning. In *Proceedings of the IEEE International Conference on Computer Vision*, pages 7464–7473, 2019. 8

[43] Du Tran, Heng Wang, Lorenzo Torresani, and Matt Feiszli. Video classification with channel-separated convolutional networks. In *Proceedings of the IEEE/CVF International Conference on Computer Vision*, pages 5552–5561, 2019. 5

[44] Aäron van den Oord, Yazhe Li, and Oriol Vinyals. Representation learning with contrastive predictive coding. *CoRR*, abs/1807.03748, 2018. 1

[45] R. Vedantam, C. L. Zitnick, and D. Parikh. Cider: Consensus-based image description evaluation. In *2015 IEEE Conference on Computer Vision and Pattern Recognition (CVPR)*, pages 4566–4575, 2015. 8

[46] Jiang Wang, Yang Song, Thomas Leung, Chuck Rosenberg, Jingbin Wang, James Philbin, Bo Chen, and Ying Wu. Learning fine-grained image similarity with deep ranking. *CoRR*, abs/1404.4661, 2014. 1, 6

[47] Liwei Wang, Yin Li, and Svetlana Lazebnik. Learning deep structure-preserving image-text embeddings. *CoRR*, abs/1511.06078, 2015. 1, 6

[48] Xinshao Wang, Elyor Kodirov, Yang Hua, and Neil Martin Robertson. Instance cross entropy for deep metric learning. *CoRR*, abs/1911.09976, 2019. 4

[49] Z. Wu, Y. Xiong, S. X. Yu, and D. Lin. Unsupervised feature learning via non-parametric instance discrimination. In *2018 IEEE/CVF Conference on Computer Vision and Pattern Recognition*, pages 3733–3742, 2018. 4

[50] Yilei Xiong, Bo Dai, and Dahua Lin. Move forward and tell: A progressive generator of video descriptions. In *ECCV*, 2018. 8

[51] Youngjae Yu, Jongseok Kim, and Gunhee Kim. A joint sequence fusion model for video question answering and retrieval. *CoRR*, abs/1808.02559, 2018. 7

[52] Youngjae Yu, Hyungjin Ko, Jongwook Choi, and Gunhee Kim. End-to-end concept word detection for video captioning, retrieval, and question answering, 2017. 7

[53] Hang Zhang, Chongruo Wu, Zhongyue Zhang, Yi Zhu, Zhi Zhang, Haibin Lin, Yue Sun, Tong He, Jonas Mueller, R Manmatha, et al. Resnest: Split-attention networks. *arXiv preprint arXiv:2004.08955*, 2020. 5

[54] Bolei Zhou, Agata Lapedriza, Aditya Khosla, Aude Oliva, and Antonio Torralba. Places: A 10 million image database for scene recognition. *IEEE Transactions on Pattern Analysis and Machine Intelligence*, 2017. 5

[55] Luowei Zhou, Chenliang Xu, and Jason J Corso. Towards automatic learning of procedures from web instructional videos. In *AAAI Conference on Artificial Intelligence*, 2018. 5

[56] Luowei Zhou, Yingbo Zhou, Jason J. Corso, Richard Socher, and Caiming Xiong. End-to-end dense video captioning with masked transformer, 2018. 8

[57] L. Zhu and Y. Yang. Actbert: Learning global-local video-text representations. In *2020 IEEE/CVF Conference on Computer Vision and Pattern Recognition (CVPR)*, pages 8743–8752, 2020. 1, 2, 7, 8